Sensors & Transducers, Vol. 262, Issue 3, September 2023, pp. 1-7

www.sensorsportal.com

Sensors & Transducers

Published by IFSA Publishing, S. L., 2023
http://www.sensorsportal.com

Polyethyleneimine-Indium Tin Oxide Composite Quartz Crystal Microbalance Sensor for Protic and Aprotic Vapors

Nirmal G. PATEL and Brian E. STADELMAIER
Department of Physics, University of North Florida
1 UNF Drive, Jacksonville, Florida 32224, USA

Received:10 August 2023 Accepted: 15 September 2023 Published: 30 September 2023

Abstract: The development of electronic noses has been an active area of research in recent years. Human sense of smell is subjective, has poor reproducibility due to such factors as fatigue and prior odors analyzed, and should not be used to detect potentially toxic chemicals. Electronic noses do not have these restrictions and offer the potential to produce reliable measurements. Electronic noses have numerous applications such as identifying toxic vapors or explosive chemicals in a warfare or factory environment, sniffing for illicit drugs, and determining food quality control and spoilage. One such electronic nose is a quartz crystal microbalance, in which a coating on a quartz crystal surface selectively interacts with vapors of interest, resulting in a change in oscillation frequency of the quartz crystal. One major category of chemical compound vapors is that they can be either protic or aprotic. In this study, we construct a quartz crystal with a nanocomposite coating that aids in determining if a vapor source is from a protic or aprotic chemical source.

Keywords: Quartz crystal microbalance, Indium tin oxide, Polyethyleneimine, Nanocomposites, Electronic nose.

1. Introduction

Polyethyleneimine (PEI) [1], as shown in Fig. 1 is a colorless, high viscosity, tacky, and hygroscopic liquid in ambient conditions.

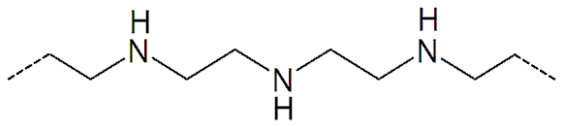

Fig. 1. Chemical structure of Polyethyleneimine $(C_2H_5N)_n$.

It is a strongly cationic or positively charged polymer. PEI is commonly used in biological research to immobilize enzymes and proteins on to inorganic substrates, and as a marker in immunology. One of us (Patel) used a polymer matrix of PEI with Poly Carbamoyl Sulfonate (PCS) hydrogel to immobilize enzymes on a platinum working electrodes to fabricate disposable biosensors for clinical and food analysis [2-5]. Based on previous experience with the formation of a matrix of PEI and PCS with a platinum electrode, we decided to create a PEI matrix with nanocrystalline ITO to enhance the performance of the ITO-QCM (Indium Tin Oxide-Quartz Crystal Microbalance) sensor. In this study, the properties of the cationic polymer PEI are combined with the properties of the nanocrystalline ITO thin film on the surface of a quartz crystal to measure protic and aprotic vapors.

A protic solvent [6] contains a hydrogen atom bound to oxygen as a hydroxyl group (OH^-), or a hydrogen atom bound to nitrogen as an amine group (RNH_2, R_2NH). More generally, any molecular solvent which contains dissociable H^+, such as hydrogen fluoride, is called a protic solvent. The

molecules of such solvents can donate an H^+ (proton). Aprotic solvents cannot donate hydrogen. Protic solvents commonly display hydrogen bonding, while aprotic solvents do not.

Fig. 2 shows the chemical structure [7] of the vapor samples used in this study with the PEI-ITO nanocomposite QCM sensor.

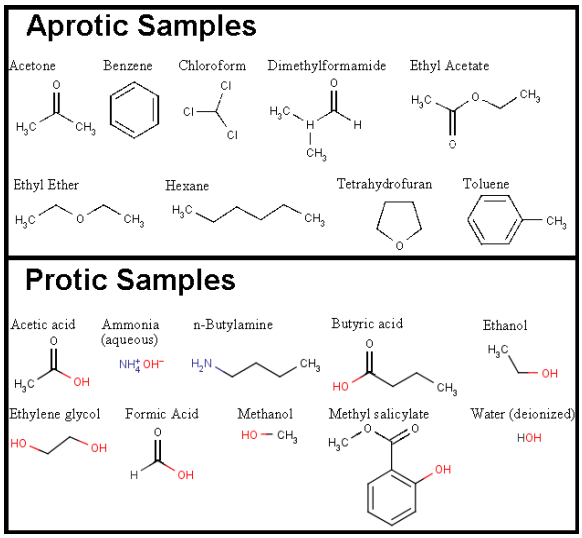

Fig. 2. Chemical structure illustrations of samples used in this study, with protic portion of molecules highlighted in red and blue.

These samples represent a random selection of some of the most common protic and aprotic solvents. These chemicals include many common flammable vapors and toxic industrial chemicals of military and homeland security interest, including those used as surrogates, simulants or chemical components of chemical agents and explosive chemicals. Regarding the importance of rapidly detecting vapors from these chemicals, we have undertaken the development of sensors for the identification of commonly available aprotic and protic group solvents.

2. Experimental

The samples chosen for this study also vary in molecular weight, vapor pressure, and polarity among both the protic and aprotic samples, as shown in Table 1 [7]. In addition, the dielectric constant is a rough measure of a solvent's polarity. Solvents with a dielectric constant of less than 15 are considered non-polar, while solvents with a dielectric constant of greater than 15 are considered polar.

Experimental details about the deposition of ITO on the quartz crystal, and structural studies of ITO films using the scanning electron microscope were reported earlier [8]. The quartz crystal microbalance (QCM) sensor in this study comprises a quartz crystal coated with a chemically sensitive PEI-ITO nanocomposite thin film. The crystal has a fundamental frequency of 5 MHz. When vapors from the sample interact with the PEI-ITO nanocomposite thin film, a change in resonance frequency is observed. The PEI-ITO nanocomposite quartz crystal was prepared by pipetting approximately 1μL of PEI onto the ITO coated portion of an AT-cut gold quartz crystal, and then spreading the liquid evenly across the surface with a polypropylene pipette tip. The PEI-ITO nanocomposite layer has an area of 1.766 cm^2 on the quartz crystal and has a shiny reflective surface, as shown in Fig. 3.

Table 1. Molecular weight, vapor pressure, and dielectric constant(κ) data of samples used in this study.

	Molecular Weight(g/mol)	**Vapor Pressure (mm Hg, 25°C)**	**Dielectric Constant (κ)**
Aprotic Samples			
Acetone	58.08	232	21
Benzene	78.11	95	2.3
Chloroform	119.38	197	4.8
Dimethylformamide	73.09	3.87	38
Ethyl Acetate	88.11	95	6
Ethyl Ether	74.12	583	4.3
Hexane	86.18	151	2
Tetrahydrofuran	72.11	150	7.6
Toluene	92.14	28.4	2.4
Protic Samples			
Acetic Acid	60.05	11	6.2
Ammonia(aqueous)	17.03(NH_3 gas)	7600 (NH_3 gas)	16.5 (NH_3 gas)
n-Butylamine	73.14	1.3	5.3
Butyric Acid	88.11	0.43	3
Ethanol	46.07	59.3	30
Ethylene Glycol	62.07	0.06	37
Formic Acid	46.02	42.6	58
Methanol	32.04	127	33
Methyl Salicylate	152.15	0.098	9
Water (deionized)	18.01	23.8	80

Fig. 3. Picture of PEI-ITO nanocomposite coated gold quartz crystal in holder.

The quartz crystal microbalance (Stanford Research Systems, Model: QCM200) was used to simultaneous measure the change in the frequency as well as the change in the surface resistance of a sensitive layer of PEI-ITO nanocomposite thin films deposited on the quartz crystal of the QCM in the presence of the sample vapor. 15 µL of either a protic or aprotic solvent was applied over one end of a 20 cm length, 2 cm width and 0.3 mm thick paper strip. The paper strip with the absorbed liquid sample was inserted immediately in the open glass jar and kept 1 cm above the surface of the PEI-ITO nanocomposite film for 20 seconds, and then removed from the jar. A digital timer was used to measure the 20 second period. A new paper strip was used for each run of each test sample. All measurements were performed in the laboratory at a temperature of approximately 21 °C and at approximately 50 % relative humidity.

3. Results and Discussion

Fig. 4 shows the average of five measurements of the PEI-ITO nanocomposite QCM sensor change in frequency for all tested samples.

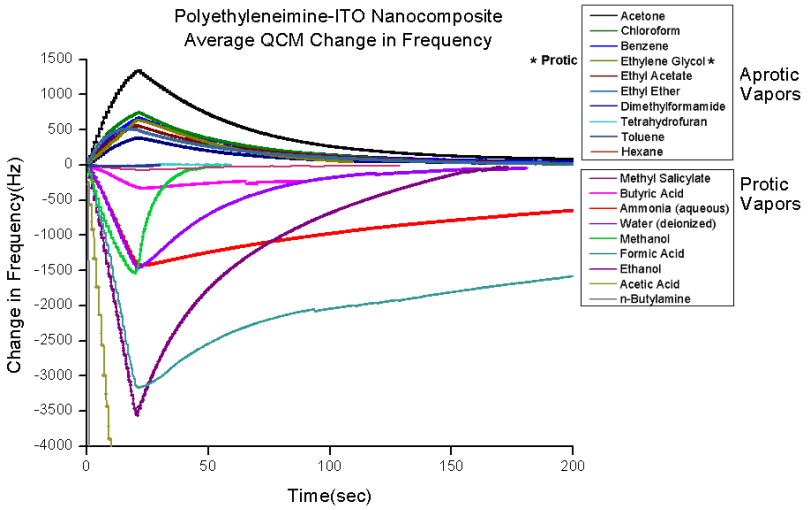

Fig. 4. Average change in frequency responses of PEI-ITO nanocomposite QCM sensor to protic and aprotic vapor samples.

Fig. 5 shows that all the protic vapor samples show an overall QCM sensor decrease in frequency, except for Ethylene Glycol. The Acetic Acid (light brown) and n-Butylamine (gray) protic vapor sample QCM decrease in frequency measurements were especially large, with only the beginning of the overall response for both samples appearing in Figs. 4 and 5.

Fig. 6 shows a graph of the aprotic sample vapor measurements that appear in Fig. 4.

Figs. 4 and 7 also show that all the aprotic vapor samples show either an overall QCM sensor increase in frequency (Acetone, Chloroform, Benzene, Ethyl Acetate, Ethyl Ether, Dimethylformamide), or a slight overall QCM decrease in frequency (Tetrahydrofuran, Toluene, Hexane).

Table 2 shows a chart of the average maximum magnitude PEI-ITO nanocomposite QCM sensor change in frequency for all samples in this study, with the protic samples highlighted in gray.

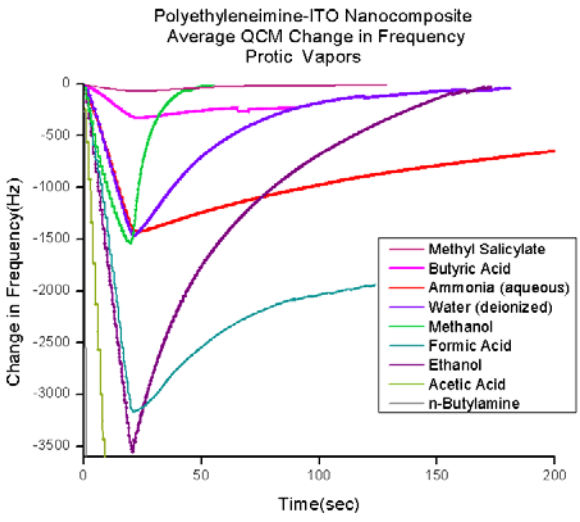

Fig. 5. Average change in frequency responses of PEI-ITO nanocomposite QCM sensor to protic vapor samples

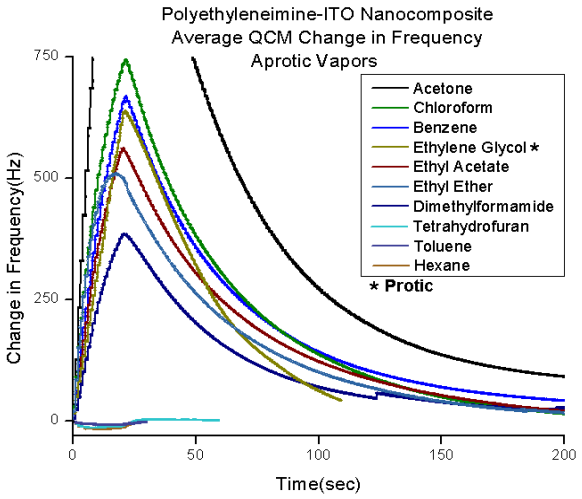

Fig. 6. Average change in frequency responses of PEI-ITO nanocomposite QCM sensor to aprotic vapor samples.

Table 2. Average maximum magnitude changes in frequency for all samples in this study.

Vapor Sample	Average of Maximum Magnitude Change in Frequency (Hz)
Acetone	1343.22
Chloroform	743.4
Benzene	667.1
Ethylene Glycol	636.0
Ethyl Acetate	560.8
Ethyl Ether	508.5
Dimethylformamide	384.6
Toluene	-6.6
Tetrahydrofuran	-13.9/+3.4
Hexane	-16.4
Methyl Salicylate	-66.7
Butyric Acid	-320.8
Ammonia(aqueous)	-1426
Water (deionized)	-1462.3
Methanol	-1535.1
Formic Acid	-3172.0
Ethanol	-3553.8
Acetic Acid	-9013.3
n-Butylamine	-3912655.7

Table 2 shows that apart from Ethylene Glycol, there is a clear separation between the protic and the aprotic vapor samples. Tetrahydrofuran showed a biphasic PEI-ITO nanocomposite QCM sensor change in frequency, in which the initial response was a decrease in frequency, then a return frequency greater than the baseline, followed by a second return to the baseline.

Fig. 7 shows the average of five measurements of the PEI-ITO nanocomposite QCM sensor change in surface resistance for all samples.

Fig. 7 shows that all the protic vapor samples show an overall QCM sensor increase in surface resistance, except for Ethylene Glycol. Fig. 8 shows a graph of just the protic sample vapor measurements (not including Ethylene Glycol) that appear in Fig. 7.

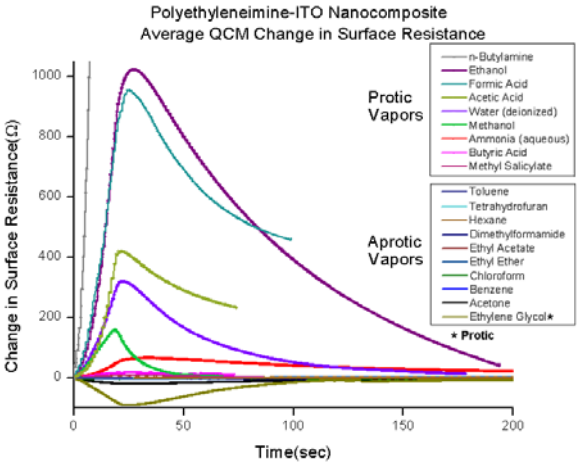

Fig. 7. Average change in surface resistance responses of PEI-ITO nanocomposite QCM sensor to protic and aprotic vapor samples.

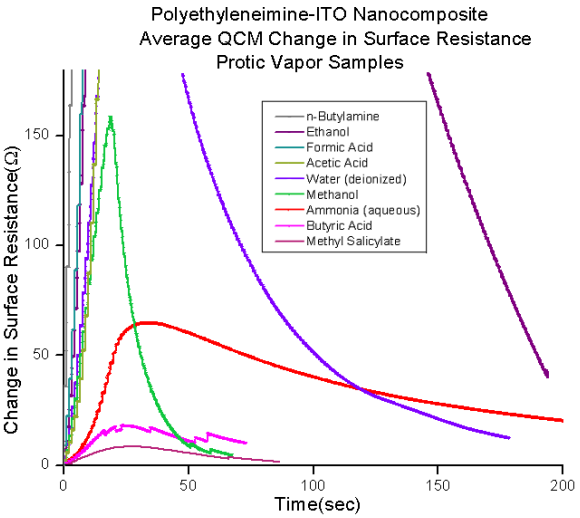

Fig. 8. Average change in surface resistance responses of PEI-ITO nanocomposite QCM sensor to protic vapor samples.

Figs. 7 and 9 (below) also show that all the aprotic vapor samples show either an overall QCM sensor decrease in surface resistance (Acetone, Chloroform, Benzene, Ethyl Acetate, Ethyl Ether, Dimethylformamide), no change in surface resistance (Hexane), or a slight overall QCM increase in surface resistance (Tetrahydrofuran, Toluene).

Table 3 shows a chart of the average maximum magnitude change in PEI-ITO nanocomposite QCM sensor change in surface resistance for all samples in this study, with the protic samples highlighted in gray.

Table 3 shows that apart from Ethylene Glycol, there is a clear separation between the protic and the aprotic vapor samples when measuring surface resistance.

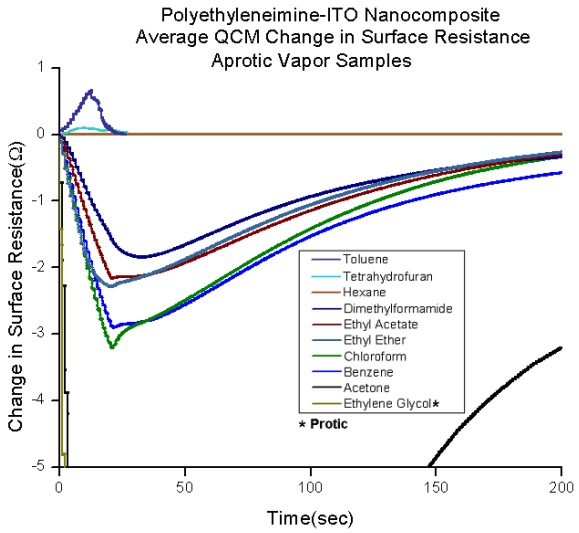

Fig. 9. Average change in surface resistance of PEI-ITO nanocomposite QCM sensor responses to aprotic vapor samples.

Table 3. Average maximum magnitude changes in surface resistance for all samples in this study.

Vapor Sample	Average of Maximum Magnitude Change in Surface Resistance (Ω)
n-Butylamine	2727.5
Ethanol	1022.2
Formic Acid	953.1
Acetic Acid	418.6
Water (deionized)	319.8
Methanol	158.3
Ammonia(aqueous)	64.9
Butyric Acid	20.3
Methyl Salicylate	8.7
Toluene	0.7
Tetrahydrofuran	0.1
Hexane	0
Dimethylformamide	-1.8
Ethyl Acetate	-2.2
Ethyl Ether	-2.3
Benzene	-2.9
Chloroform	-3.2
Acetone	-18.2
Ethylene Glycol	-91.2

Regarding a theoretical explanation for the observed PEI-ITO nanocomposite QCM sensor changes in surface resistance observed with the protic vapors, an increase in surface resistance corresponds to an increase in viscoelasticity or softening of the PEI-ITO. Nanocrystalline grains of 1000Å thick ITO films are cross-linked with the PEI polymer to form a nanocomposite matrix layer on the surface of the quartz crystal. The protic vapors are temporarily softening the nanocomposite matrix of PEI and nanocrystalline ITO by dissolving the PEI during exposure to the sample vapor, causing it to swell and soften. We need to perform a surface analysis of our PEI-ITO nanocomposite QCM sensor under the low vacuum mode of our environmental scanning electron microscope to confirm this. Our hypothesis is based on reported work by Barth and Rademann [9] on the cross-linking of polyethyleneimines ultraresins. They reported that swelling in protic solvents is very high for free amine resins, especially in water, and is further increased at lower pH.

Regarding a theoretical explanation for the observed PEI-ITO nanocomposite QCM sensor changes in surface resistance observed with the aprotic vapors, a decrease in surface resistance corresponds to a decrease in viscoelasticity or stiffening of the PEI-ITO. The aprotic sample vapors are apparently dehydrating the hygroscopic PEI to some degree, causing it to stiffen. This explanation is supported by earlier published works [10-11]. Sharata and Burnette [10] used aprotic solvents to dehydrate biological tissues. Tsoleridis et al. [11] reported that dehydration is facilitated by the ability of aprotic solvents, in contrast to protic solvents, to carry away water formed during chemical reactions.

Regarding why Ethylene Glycol shows an opposite PEI-ITO nanocomposite QCM sensor change in frequency and surface resistance compared to the other protic samples, since Ethylene Glycol is a strong desiccant unlike all of the other protic samples, and since PEI is known to be hygroscopic [12], it is likely that the Ethylene Glycol may be desorbing water from the PEI on the quartz crystal surface during the sample measurement period. If water is desorbed from the PEI-ITO nanocomposite matrix on the quartz crystal surface, that would decrease its overall viscoelasticity, or make it stiffer. A decrease in viscoelasticity or a stiffening of the PEI-ITO nanocomposite coating on the quartz crystal surface would be measured as a PEI-ITO nanocomposite QCM sensor decrease in surface resistance, which is observed with the Ethylene Glycol sample.

Fig. 10 shows the average maximum change in frequency of the PEI-ITO nanocomposite quartz crystal as a function of the molecular weights of the protic and aprotic samples in this study.

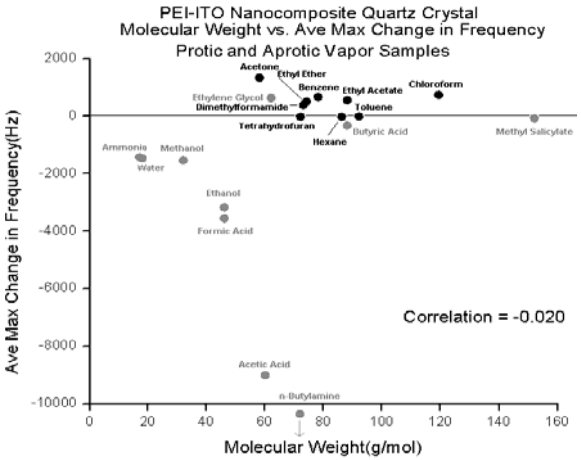

Fig. 10. Average PEI-ITO QCM sensor maximum change in frequency vs. molecular weight for samples in this study (protic samples in gray).

The correlation coefficient between the average maximum change in frequency and molecular weight of each of the samples in Fig. 7 is about -0.020, which indicates that the average maximum change in frequency is not dependent on the molecular weight of the samples. Fig. 10 shows that adding PEI to ITO to form a nanocomposite sensor makes its change in frequency response to sample vapors independent of the sample's molecular weight.

Figs. 11a and 11b show the average maximum changes in frequency and surface resistance as a function of the dielectric constants of the protic and aprotic samples in this study.

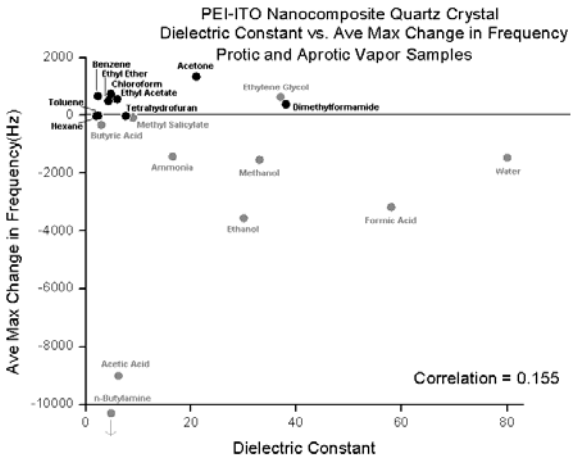

Fig. 11a. Average PEI-ITO QCM sensor maximum changes in frequency vs. dielectric constant for samples in this study (protic samples in gray).

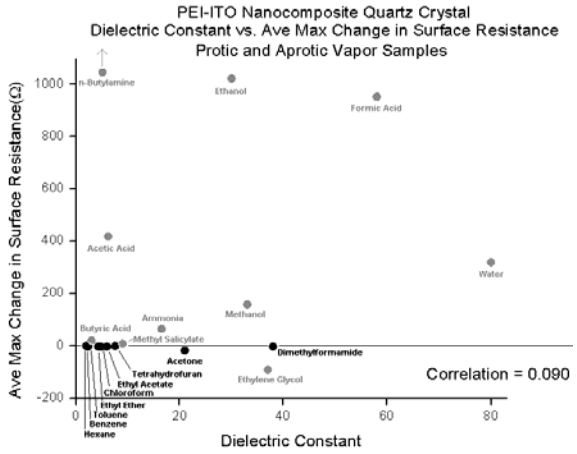

Fig. 11b. Average PEI-ITO QCM sensor maximum changes surface resistance vs. dielectric constant for samples in this study (protic samples in gray).

The correlation coefficient between the average maximum change in frequency and the dielectric constant of each of the samples in Fig. 11a is about 0.155, while the correlation coefficient between the average maximum change in surface resistance and the dielectric constant of each of the samples in Fig. 11b is about 0.090, which indicates that neither the average maximum change in frequency nor the average maximum change in surface resistance is dependent on the dielectric constant.

4. Conclusions

The PEI-ITO nanocomposite QCM sensor was sensitive to the sample vapors in this study. The PEI-ITO nanocomposite QCM sensor showed an increase in frequency response with 6 out of 9 aprotic sample vapors, with the other 3 aprotic sample vapors all showing a small decrease in frequency response relative to 9 out of the 10 protic samples. The PEI-ITO nanocomposite coated quartz crystal's changes in frequency responses and surface resistance were independent of both the sample's molecular weight and polarity based on the dielectric constant. The PEI-ITO nanocomposite QCM sensor displayed an impressive, though less than perfect ability to distinguish between most protic and aprotic sample vapors. A PEI-ITO nanocomposite QCM sensor could be utilized in an electronic nose sensor array to aid distinguishing protic from aprotic vapors.

Acknowledgements

The authors are grateful to the U.S. Army, Edgewood Chemical Biological Center, Aberdeen Proving Ground, MD, USA (now DEVCOM CBC), Department of Defense for their financial support.

References

[1]. https://polymerdatabase.com/Polymer Brands/Polyethyleneimine.html

[2]. N. G. Patel, A. Erlenkotter, K. Cammann, G. C., Chemnitius, A biosensor for the detection of lactic acid, *India patent 196514*, June 24, 2005.

[3]. N. G. Patel, A. Erlenkotter, K. Cammann, G. C. Chemnitius, Fabrication and characterization of disposable type lactate oxidase sensors for dairy products and clinical analysis, *Sensors and Actuators B: Chemical*, Vol. 67, Issues 1–2, August 10, 2000, pp. 134-141.

[4]. N. G. Patel, S. Meier, K. Cammann, G. C. Chemnitius, Screen-printed biosensors using different alcohol oxidases, *Sensors and Actuators B: Chemical*, Vol. 75, Issues 1–2, April 30, 2001, pp. 101-110.

[5]. U. B. Trivedi, D. Lakshminarayan, I. L. Kothari, N. G. Patel, Potentiometeric biosensor for urea determination in milk, *Sensors and Actuators B: Chemical*, Vol. 140, Issue 1, June 18, 2009, pp. 260-266.

[6]. J. R. Rumble, Laboratory Solvent Solvents and Other Liquid Reagents, CRC Handbook of Chemistry and Physics, 102nd Edition, Internet Version. *Taylor & Francis*, 2021.

[7]. http://www.chemspider.com/

[8]. N. G. Patel, J. Huebner, J. Saredy, B. E. Stadelmaier, Odor Sensing with Indium Tin Oxide Thin Films on Quartz Crystal Microbalance, *Sensors & Transducers*, Vol. 91, Issue 4, April 2008, pp. 116-126.

[9]. M. Barth and J. Rademann, J. Comb, Tailoring ultaresins based on the cross-linking of polyethyleneimines, *J. Comb. Chem.*, Vol. 6, 3, March 13, 2004, pp. 340–349.
[10]. H. H. Sharata, R. Ronald R. J. Burnette, Effect of dipolar aprotic permeability enhancers on the basal stratum corneum, *Journal of Pharmaceutical Sciences*, Vol. 77, Issue 1, Jan. 1988, pp. 27-32.
[11]. D. Hatzimimikou, C. Neochoritis, M. A. Terzidis, A. Constantinos, A. Tsoleridis, J. Stephanidou-Stephanatou, D. Livadiotou,. A Versatile One-Pot Synthesis of β-Carbolines by Reaction of Pyranoindolones with Phenyl- and Benzoylhydrazine, *Synthesis*, Vol. 20, Oct. 2008, pp. 3273-3278.
[12]. G. M. J. Slusarczuk, R. E. Brooks, Ferrite Flocculating System, *US Patent 4,193,866*, Mar. 18, 1980.